Aerosol Science and Technology

Nature of Sub-23-nm Particles Downstream of the European Particle Measurement Programme (PMP)-Compliant System: A Real-Time Data Perspective

Zhongqing Zheng [a] [b] , Thomas D. Durbin [a] , Georgios Karavalakis [a] , Kent C. Johnson [a] , Ajay Chaudhary [a] , David R. Cocker III [a] , Jorn D. Herner [c] , William H. Robertson [d] , Tao Huai [e] , Alberto Ayala [e] , David B. Kittelson [f] & Heejung S. Jung [a] [b]

[a] Center for Environmental Research and Technology (CE-CERT), Bourns College of Engineering, University of California, Riverside, Riverside, California, USA

[b] Department of Mechanical Engineering, University of California, Riverside, Riverside, California, USA

[c] Research Division, California Air Resources Board (CARB), Sacramento, California, USA

[d] Mobile Source Control Division, California Air Resources Board (CARB), Sacramento, California, USA

[e] Monitoring and Laboratory Division, California Air Resources Board (CARB), Sacramento, California, USA

[f] Department of Mechanical Engineering, University of Minnesota, Minneapolis, Minnesota, USA

Available online: 13 Jun 2012

PLEASE SCROLL DOWN FOR ARTICLE

Nature of Sub-23-nm Particles Downstream of the European Particle Measurement Programme (PMP)-Compliant System: A Real-Time Data Perspective

Zhongqing Zheng,[1,2] Thomas D. Durbin,[1] Georgios Karavalakis,[1] Kent C. Johnson,[1] Ajay Chaudhary,[1] David R. Cocker III,[1] Jorn D. Herner,[3] William H. Robertson,[4] Tao Huai,[5] Alberto Ayala,[5] David B. Kittelson,[6] and Heejung S. Jung[1,2]

[1]*Center for Environmental Research and Technology (CE-CERT), Bourns College of Engineering, University of California, Riverside, Riverside, California, USA*

[2]*Department of Mechanical Engineering, University of California, Riverside, Riverside, California, USA*

[3]*Research Division, California Air Resources Board (CARB), Sacramento, California, USA*

[4]*Mobile Source Control Division, California Air Resources Board (CARB), Sacramento, California, USA*

[5]*Monitoring and Laboratory Division, California Air Resources Board (CARB), Sacramento, California, USA*

[6]*Department of Mechanical Engineering, University of Minnesota, Minneapolis, Minnesota, USA*

This study provides an evaluation of the nature of sub-23-nm particles downstream of the European Particulate Measurement Programme (PMP) methodology, with prescribed cycles and on-road flow-of-traffic driving conditions. Particle number concentrations and size distributions were measured using two PMP measurement systems running simultaneously. For this analysis, the focus is on the real-time results from multiple instruments. The results revealed that a significant fraction of particles downstream of both PMP systems for all tested cycles were below 11 nm. The fraction of sub-11-nm particles observed downstream of the PMP system decreased when the overall dilution ratio of one PMP system was increased from 300 to 1500, suggesting those sub-11-nm particles were formed through re-nucleation of semivolatile precursors. When the evaporation tube temperature was increased from 300°C to 500°C, no difference in particle number concentrations was observed, suggesting that incomplete evaporation of semivolatile particles did not contribute to those sub-11-nm particles. Particle emissions were about one order of magnitude higher during flow-of-traffic driving along a highway with a steep grade than during the prescribed driving cycles. During the same flow-of-traffic condition, a sudden jump in PMP operationally defined solid particle concentration was observed, while the accumulation mode particle concentrations in the constant volume sampling (CVS) tunnel measured by an engine exhaust particle sizer (EEPS) only showed a slight increase. This discrepancy was attributed to the extensive growth of the re-nucleated particles downstream of the PMP systems.

1. INTRODUCTION

The most prominent sources of particles in urban environments are vehicular emissions and secondary photochemical reactions. While heavy-duty diesel vehicles constitute only a small fraction of the total fleet in California (CA) and the United States, diesel particulate mass contributes significantly to urban air pollution and has been associated with adverse health effects (EPA 2002; Li et al. 2009). Standards for vehicle particulate matter (PM) emissions in the US are presently based on mass, while particle number emissions are not regulated directly. With the introduction of more stringent emission standards and newer control technologies, such as diesel particle filters (DPFs), as well as new fuel and oil formulations, PM mass emissions are close to minimum measurement sensitivity levels. PM mass measurements can also suffer from large uncertainties due to artifacts, such as those caused by gaseous or semivolatile emissions (Chase et al. 2004; Burtscher 2005; Swanson et al. 2009).

A methodology for the measurement of particle number emissions has been developed within the framework of the Particle Measurement Programme (PMP), in which only non-volatile, solid particles are measured (Andersson et al. 2007). The protocol is now formally a part of the Euro 5 and subsequent standards. This specific protocol was designed to measure solid particles with a diameter above 23 nm because the measurement of nonvolatile particles is more repeatable from a practical point of view (Giechaskiel et al. 2008), and the original PMP protocol was designed assuming standards would be met using high-efficiency exhaust filters that are equally or even more efficient in removing sub-23-nm particles than particles larger than 23 nm. Volatile particles are removed through thermal treatment using a volatile particle remover (VPR), leaving particles that are operationally defined as solid, to be counted by a condensation particle counter (CPC) with a 50% counting efficiency for 23-nm particles.

Solid particles in the sub-23-nm size range have been found in heavy-duty diesel vehicle exhaust under different load conditions (Kittelson et al. 2006; Herner et al. 2007; Rönkkö et al. 2007; Filippo and Maricq 2008; Lähde et al. 2009; Lähde et al. 2010). These findings raise questions as to whether excluding the sub-23-nm particles is appropriate or necessary. Understanding the nature of these sub-23-nm particles, whether they are volatile or solid, is important from a regulatory, scientific, health, and environmental perspective. The fact that a significant number of sub-23-nm solid particles can be present in diesel exhaust and that they can be measured practically suggests that further investigation of the current method is necessary.

The debate about the 23-nm cutoff diameter of the PMP protocol has drawn several studies to investigate the nature and number concentration levels of sub-23-nm particles downstream of the PMP, including the PMP heavy-duty interlaboratory correlation exercise (ILCE_HD). Johnson et al. (2009) reported that the particle number concentration of sub-23-nm particles downstream of the PMP system was about an order of magnitude higher than that of particles larger than 23 nm for a continuously regenerating trap (CRT^{TM})-equipped heavy-duty diesel vehicle operating over different cycles, such as European Transient Cycle, California Air Resources Board creep cycle, and Urban Dynamometer Driving Schedule. Giechaskiel et al. (2009) showed that the concentrations of sub-23-nm solid particles were 15–45% higher than those of the solid particles above the 23-nm threshold over various testing cycles. However, a difference as large as 85% between the concentrations of sub-23-nm and above-23-nm particles was observed for the cold-start of the World Harmonized Transient Cycle (WHTC) by the PMP ILCE_HD (Andersson et al. 2010). Dwyer et al. (2010) showed that the difference between sub-23-nm and above-23-nm particle concentrations can vary by two orders of magnitude for the same cycle with DPF regeneration for a light-duty diesel vehicle. The foregoing discussion and other studies have demonstrated the difficulties in achieving good repeatability and reproducibility for particles smaller than 23 nm (Andersson et al. 2010),

which is one of the reasons the sub-23-nm particle fraction was excluded from the PMP measurement to begin with.

This study presents a unique study to evaluate the performance of the PMP methodology over a wide range of on-road driving conditions. This paper aims to evaluate the PMP methodology based on real-time data to answer the following questions: (1) How do sub-23-nm particle concentrations vary over different testing conditions? (2) What is the nature of sub-23-nm particles? Embedded in the answers to these questions is a suggestion that with currently available instrumentation, such as CPCs with cutoff diameters smaller than 23 nm, the fraction of the emission aerosol that are smaller than 23 nm can be measured and, hence, evaluated. Findings from this study also provide information on why it is difficult to obtain repeatable sub-23-nm particle measurements with the PMP protocol, on instrument comparisons, and on the nuances of constant volume sampling (CVS) and the two PMP systems. This is a companion paper to Johnson et al. (2009), which describes cycle-integrated PM mass and PM number concentrations for the same experiments reported in this study. The current paper provides an in-depth evaluation of the real-time data and a more detailed explanation of the aerosol phenomena.

2. EXPERIMENTAL APPROACH

2.1. Test Vehicle, Fuels, and Lubricants

The test vehicle was the Bourns College of Engineering-Center for Environmental Research and Technology (CE-CERT)'s in-house Freightliner Class 8 truck, equipped with a 2000 Caterpillar C-15 engine (14.6 L, 6 cylinders, and 475 hp). This vehicle is certified to EPA 2000 model year standards, with an NO$_x$ certification level of 3.7 g/bhp-h and a PM certification level of 0.08 g/bhp-h.

For this study, the vehicle was retrofitted with a Johnson Matthey CRT^{TM}. The CRT^{TM} is a passive, wall-flow-type DPF, which regenerates continuously when the exhaust temperature is above ~250°C. Platinum is used in the first chamber of the CRT^{TM} as the catalyst to oxidize NO to NO$_2$. The mileage accumulated on the DPF was about 2700 miles prior to this study.

The vehicle had a mileage of 18,000 miles and was loaded by CE-CERT's Mobile Emissions Laboratory (MEL) trailer, which included all the emissions analyzers. The weight of the tractor and the MEL was 65,000 lbs. Emission tests were conducted using California Air Resources Board (CARB) ultra-low sulfur diesel (ULSD) fuel (S < 15 ppm). The lubrication oil used was an SAE 15W-40 formulation, with a sulfated ash content of 1.35% by weight.

2.2. Test Cycles

Testing was performed on road using the motorway segment of the European Transient Cycle (ETC), the Urban

Dynamometer Driving Cycle (UDDS), and two flow-of-traffic tests. The ETC motorway cycle is a highway cruise cycle with a speed of approximate 50 miles per hour (mph). The cycles were conducted on highways and farm roads near Thermal, CA, in the Palm Springs/eastern Coachella Valley area of California. This area is remote, lightly trafficked, and, hence, makes for a suitable test track for vehicle emissions testing. Descriptions of the ETC and UDDS cycles are provided in the Supplemental Information of the companion paper, Johnson et al. (2009). Note that the UDDS cycle results presented in this paper represent only the first 700 s of the cycle and there was a break during one of the UDDS tests due to limitations on the length of the test road. The average speed of the first 700 s of the UDDS was ∼8 mph. For the ETC motorway cycle, the vehicle was accelerated to reach a cruise speed of 50 mph prior to starting the cycle. The flow-of-traffic test denoted as route 1 was conducted under freeway driving conditions that included long climbs in elevation (grade of 2.9%, defined as the ratio of rise to run), where the engine was subjected to higher loads than those in the standard cycles. The route 2 flow-of-traffic test was conducted on a long arterial road, with stops about every 2 miles.

2.3. PMP Measurement Systems

Two PMP measurement systems were used for this study. One, which is denoted as PMP system-A, was assembled to clone the first commercially available PMP measurement system at the time (circa 2007) when these experiments were performed. The PMP system-A is composed of a preclassifier/cyclone sampling directly from the CVS tunnel with a 2.5-μm size cut, a volatile particle remover (VPR) for volatile species control, and a CPC (TSI 3790) with a 23-nm cutoff diameter. The VPR includes an initial hot dilution (150°C) stage with a rotating disk-type diluter (MD-19, Matter Engineering), followed by an evaporation tube (ET) heated to a 300°C wall temperature, followed by a second diluter (ejector diluter, Dekati) at room temperature. The sequence of hot dilution, followed by an ET, and then cold dilution is designed to lower volatile concentrations and to suppress re-nucleation. The primary and secondary dilution ratios of the PMP system-A were 30:1 and 10:1, respectively, during the ETC cycle. For the UDDS cycle, the primary dilution ratio was varied between 30:1 and 150:1, while the secondary dilution was fixed at 10:1. The ET temperature was maintained at 300°C for all test cycles.

The other PMP system, denoted as PMP system-B, was designed to provide a comparison with the PMP system-A. The PMP system-B utilizes a modified design of an ISO 8178 partial flow single venturi fractional flow sampler (Figure 1). The venturi creates a negative pressure, causing the sample to flow from the CVS to the ET. A Swagelok® tee, which serves as the first particle number diluter (PND1), was placed upstream of the ET. Both the heated dilution air (150°C) and exhaust sample were introduced into the tee by the negative pressure created by the venturi. The mixed flow of dilution air and exhaust sample then flowed into the ET and the venturi, which serves as the second particle number diluter (PND2). The ET maintained a residence time of 0.2 s. The flow rate of the clean air into the venturi was 100 liter per minute (Lpm), resulting in a 10-Lpm flow through the ET, as determined by calibration. Therefore, the dilution ratio of PND2 was 11:1. The flow rate of the PND1 dilution air was controlled at 9 Lpm so that the exhaust sample flowing into the tee was 1 Lpm, making the dilution ratio of PND1 to be 10:1. The ET temperature of the PMP system-B was maintained at 300°C for the ETC motorway cycle and the two flow-of-traffic tests, and was varied between 300°C and 500°C for the UDDS cycles. PMP system calibrations according to the regulations (i.e., UNECE Regulation 49 and Regulation 83) were not performed because the regulations were yet to be published at the time of testing. All CPCs, however, were calibrated following CPCs' manuals to assure measurement quality (Durbin et al. 2008).
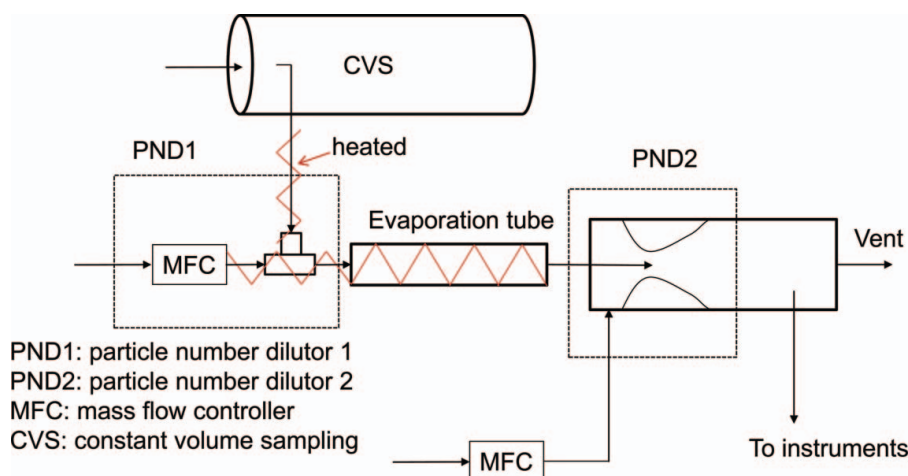

FIG. 1.   Schematic diagram of the PMP system B. (Color figure available online.)

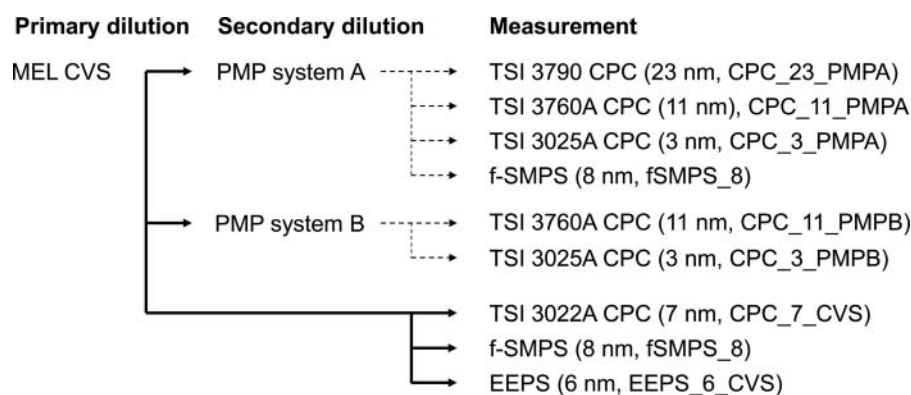**Primary dilution**   **Secondary dilution**   **Measurement**

FIG. 2.   Flow diagram of PM sampling system off the primary dilution tunnel. Solid and dotted lines show measurement off the primary and secondary dilution, respectively. Numbers within parentheses are D50 cutoff diameter of the instruments. The fSMPS was switched between both the CVS and the PMP systems.

CPCs with different cutoff diameters were used below the PMP system-B, as shown in Figure 2. Three CPCs were sampling on the PMP system-A; they were a TSI 3790 CPC with a cutoff diameter of 23 nm (labeled as CPC_23_PMPA), a TSI 3760A CPC with a cutoff diameter of 11 nm (labeled as CPC_11_PMPA), and a TSI CPC 3025A with a cutoff diameter of 3 nm (labeled as CPC_3_PMPA). Since only a single TSI 3790 CPC was available for this project, the PMP system-B utilized a TSI 3760A (labeled as CPC_11_PMPB) and a TSI 3025A (labeled as CPC_3_PMPB) for particle number measurements.

Additional measurements were also made at the CVS using an engine exhaust particle sizer (EEPS) with a lower size cut of 6 nm (labeled as EEPS_6_CVS) and a TSI 3022A CPC with a cutoff diameter of 7 nm (labeled as CPC_7_CVS) to measure particle size distributions and number concentrations. A fast

scanning mobility particle sizer (fSMPS) with a lower size cut of 8 nm (labeled as fSMPS_8) (Shah and Cocker 2005) was switched between the CVS and the PMP system-A to measure particle size distributions.

3. RESULTS

3.1. Particle Size Distributions and Particle Number Concentrations in the CVS

As the PMP systems sample from the CVS, it is important to characterize the CVS aerosol. Figures 3a and b show the results of particle measurements made for the ETC motorway cycle. Figure 3a shows particle size distribution contours measured with the fSMPS_8 while Figure 3b shows total number concentrations measured in the CVS tunnel with the EEPS_6_CVS and CPC_7_CVS, as well as particle number measurements made
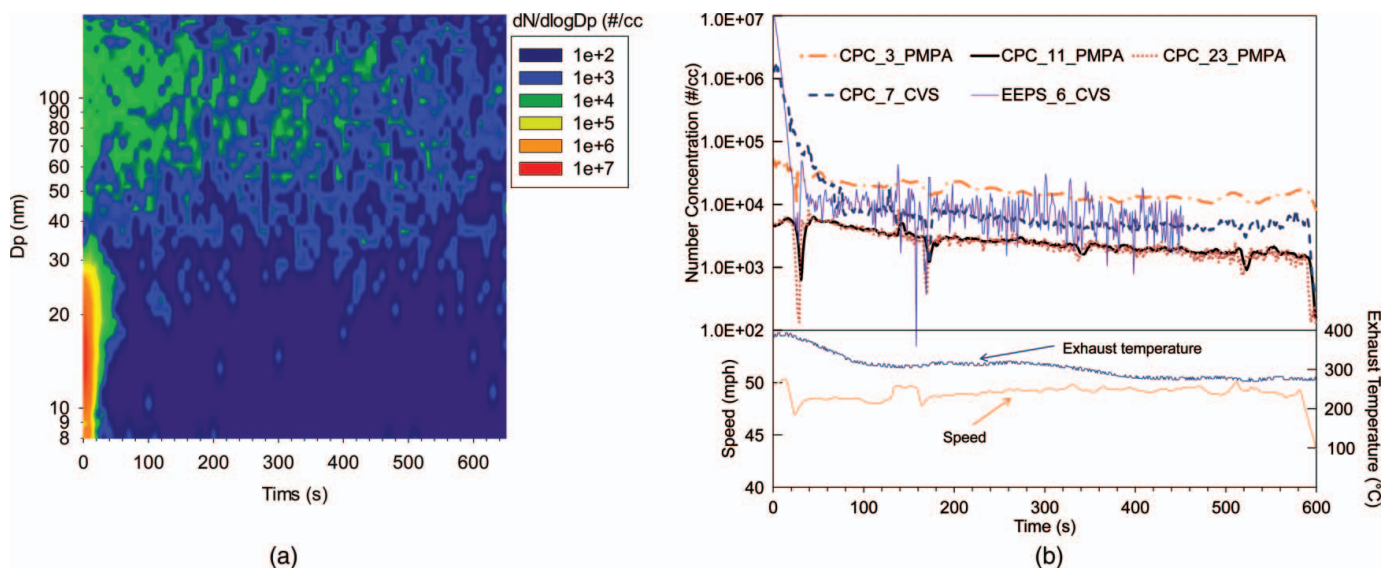

FIG. 3.   Particle concentrations and size distributions for the ETC motorway cycle: (a) particle size distribution spectrum at the CVS measured by the fSMPS; (b) particle concentrations measured by CPCs along with exhaust temperature. (Color figure available online.)

downstream of the PMP system-A with the CPC_23_PMPA, CPC_11_PMPA, and CPC_3_PMPA. Exhaust temperature and vehicle speed are also shown. For this cycle, the test vehicle was accelerated to reach a cruise speed of 50 mph prior to the beginning of the ETC motorway cycle, resulting in the higher exhaust temperature at the start (t = 0) of the cycle. The accumulation mode particles are at their highest level at the start of the cycle and gradually decrease throughout the test, as may be seen from the fSMPS_8_CVS data in the 40–200-nm range. The fSMPS_8_CVS data show initial formation, followed by quick decay of a nucleation mode in the CVS tunnel, in the 8–30 nm region. This is also apparent in Figure 3b in the EEPS_6_CVS and CPC_7_CVS data. For most of the first ∼80 s of the test, CPC_7_CVS reads higher than EEPS_6_CVS. The lower counting limit of the EEPS_6_CVS (TSI Model EEPS 3090) is 5.6 nm, and it counts nothing below that size. On the other hand, the CPC_7_CVS (TSI model CPC 3022A) has a broad counting efficiency curve and a 10% nominal counting efficiency for 4-nm particles. The higher counts with the CPC_7_CVS suggest a nucleation mode with significant particle concentrations below 6 nm. This is consistent with the results shown by Zheng et al. (2011), where they found a significant number of particles between 3 nm and 7 nm in the CVS by comparing various CPCs with different cutoff diameters, all sampling directly from the CVS.

The formation of a semivolatile nucleation mode, as measured at the CVS, is most likely due to SO_2 to SO_3 conversion over the DPF. This conversion is temperature dependent, with higher conversion found for higher temperatures (Herner et al. 2011). Figure 3b shows a decrease in exhaust temperature with time, and this is associated with a reduction in the concentration of the nucleation mode particles. The slow decrease of the CPC_7_CVS concentration tracks the exhaust temperature curve.

Results of the UDDS cycle are shown in Figure 4. Particle size distribution spectra of the fSMPS_8, shown in Figure 4a, reveal the dominance of accumulation mode particles. Since it is likely that most of the particles in the accumulation mode are solid, and since the fSMPS_8_CVS data show no significant particles between 8 nm and 11 nm, the differences between the CPC_7_CVS and CPC_11_PMPA data (Figure 4b) suggest the presence of sub-8-nm nucleation mode particles in the CVS for the UDDS cycle, similar to the ETC motorway cycle. It should be noted that there was a discontinuation at about t = 300 s for this UDDS cycle due to a stop sign on the testing road.

Figure 5a shows particle size distributions measured with the EEPS_6_CVS in the CVS for the route 1 flow-of-traffic test. The route 1 flow-of-traffic test had a number of long climbs in elevation, so the average engine load on the route 1 was higher than that of the UDDS or ETC motorway cycle. The total particle number emissions were dominated by the nucleation mode particles after about 50 s, when the exhaust temperature exceeded 350°C, as shown in Figure 5b. The CPC_7_CVS was saturated throughout the entire test due to the high concentration of nucleation mode particles in the CVS, so these data are not shown. The EEPS was also saturated between about 11 nm and 26 nm, so concentrations shown in this range are underestimated.

3.2. Particle Number Concentrations Downstream of the PMP Systems

Particle number concentrations downstream of the PMP systems are shown in Figures 3b, 4b, and 5b, for the ETC motorway cycle, the UDDS cycle, and the route 1 flow-of-traffic test, respectively. Particle number concentrations downstream of the
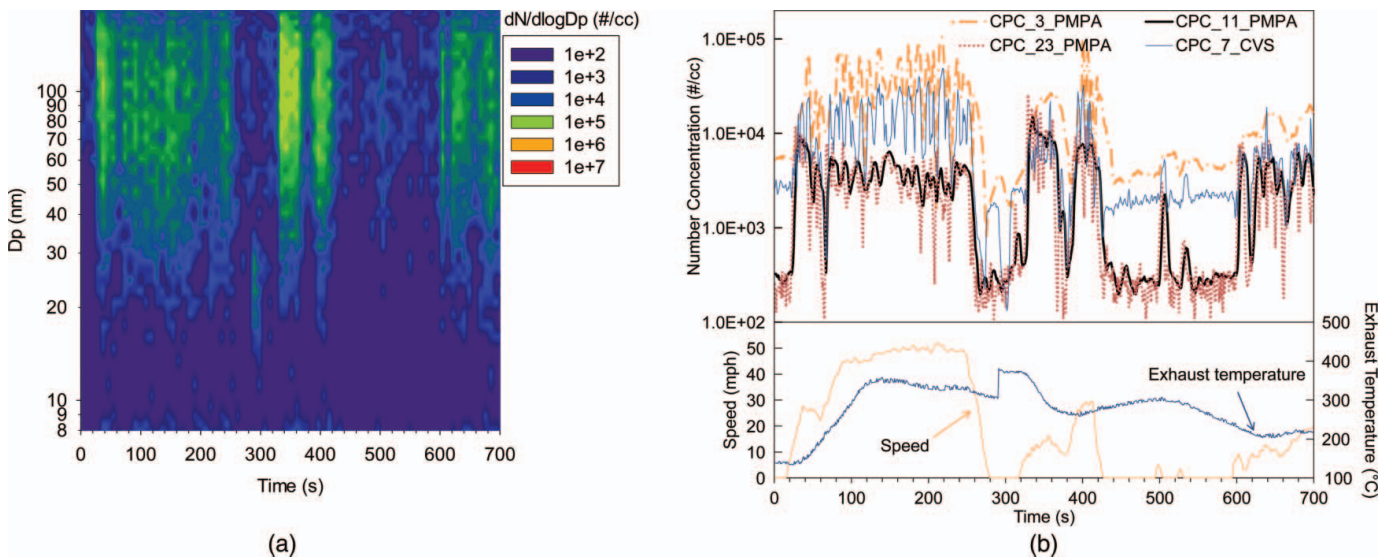

FIG. 4.   Particle concentrations and size distributions for the UDDS cycle: (a) particle size distribution spectrum at the CVS measured by the fSMPS_8; (b) particle concentrations measured by different CPCs. (Color figure available online.)
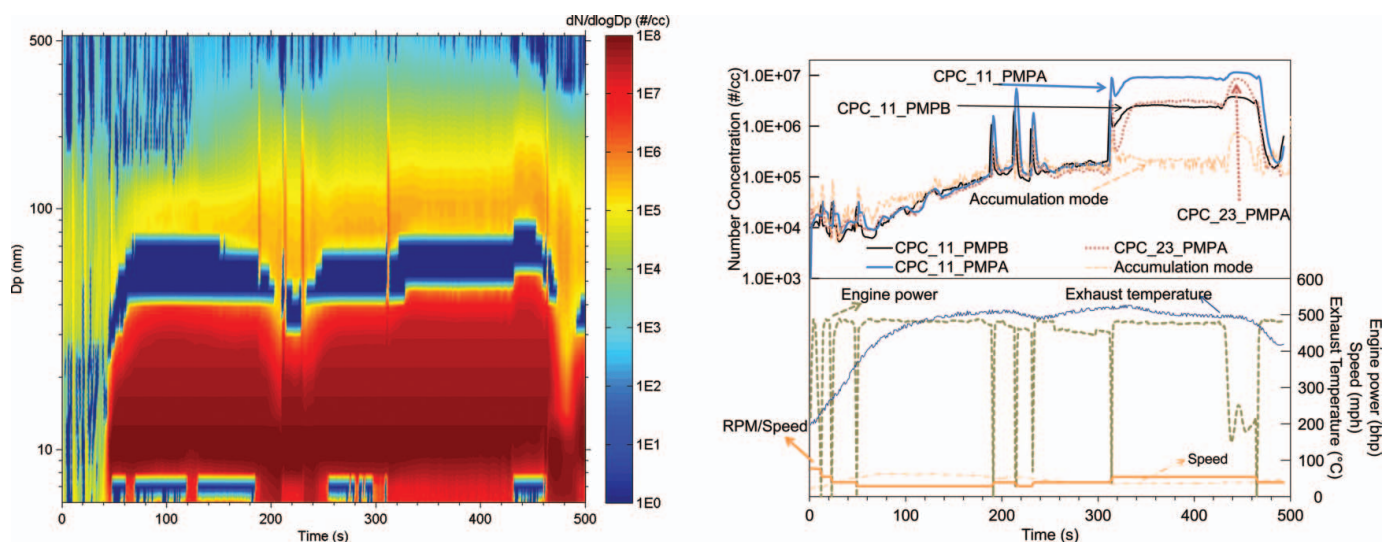
FIG. 5. Particle concentration and size distributions during flow-of-traffic (route 1): (a) particle size distributions spectrum at the CVS measured by the EEPS_6_CVS; (b) particle concentrations measured by CPCs along with exhaust temperature and engine power. (Color figure available online.)

PMP systems were all corrected for dilution ratio to reflect the concentrations that would be seen in the CVS.

During the ETC motorway cycle, as shown in Figure 3b, the CPCs downstream of the PMP system-A showed a significant number of particles below 11 nm. This can be seen by the nearly one order of magnitude higher concentrations for the CPC_3_PMPA compared with those of the CPC_11_PMPA and CPC_23_PMPA. The CPC_11_PMPA and CPC_23_PMPA tracked each other very well, indicating there was a negligible number of particles between 11 nm and 23 nm, the respective cutoff diameters of the two CPCs.

During the UDDS cycle, the CPCs that measured particle concentrations downstream of the PMP systems, as shown in Figure 4b, gave results similar to those of the ETC motorway cycle. The CPC_3_PMPA measured $\sim$3–30 times higher concentrations than the CPC_11_PMPA and CPC_23_PMPA, showing that most of particles present were smaller than 11 nm. The CPC_11_PMPA and the CPC_23_PMPA tracked each other very well, showing no, or negligible, particles of sizes between 11 nm and 23 nm. The differences between the CPC_3_PMPA, the CPC_11_PMPA, and the CPC_23_PMPA varied, and seemed to be smaller when the accumulation mode was more prominent (e.g., t = 350 – 450 s). This is consistent with suppression of nucleation by adsorption onto the accumulation mode particles.

Although particle number concentrations downstream of the PMP system-B are not presented for the ETC motorway and the UDDS cycles to reduce the complexity of the figures, it is worth mentioning that particle number concentrations downstream of the PMP system-B were similar to those downstream of the PMP system-A. Specifically, the CPC_3_PMPB concentrations agreed well with those for the CPC_3_PMPA for both the ETC motorway and the UDDS cycles, and the CPC_11_PMPB concentrations agreed well with the CPC_11_PMPA concentrations.

The agreement between the two PMP systems suggests that the performance of the PMP is insensitive to the dilution method employed.

Figure 5b shows particle number concentrations downstream of the PMP systems during the route 1 flow-of-traffic test. Particle concentrations were orders of magnitude higher than those from the standard driving cycles (i.e., the ETC motorway cycle and the UDDS) presented earlier in this section. Only the three high cutoff diameter CPCs, i.e., the CPC_11_PMPA, the CPC_23_PMPA, and the CPC_11_PMPB, are shown in the figure because both the CPC_3_PMPA and the CPC_3_PMPB were saturated throughout the test. The saturation of the low cutoff diameter CPCs (i.e., the CPC_3_PMPA and the CPC_3_PMPB) indicates very high concentrations of sub-11-nm particles downstream of both the PMP systems. The integrated particle number emissions as measured by the CPC_11_PMPA, the CPC_23_PMPA, and the CPC_11_PMPB were 2.3×10^{12}, 9.7×10^{11}, and 1.5×10^{12} particles/kWh, respectively. Even the high cutpoint CPCs (i.e., the CPC_11_PMPA, the CPC_23_PMPA, and the CPC_11_PMPB) were saturated for about 140 s, from t = 320 s to t = 460 s during the route 1 test, so that this time window was excluded from the emission calculation.

Particle concentrations showed a steady increase from t = 60 s to t = 180 s, while the engine load is nearly constant. This is likely due to the gradual decrease of the DPF filtration efficiency, which is in turn due to the consumption of the soot cake as the DPF regenerates. There were a few spikes at about t = 190, 210, 230, and 320 s, which tracked well with vehicle gear shifts. From t = 230 s to t = 320 s, particle concentrations were relatively steady and in the range of 10^5 particles/cm^3. Note the 10^5 particles/cm^3 is PMP dilution corrected, and as such, is still one order of magnitude lower than the saturation levels of the instruments.

Accumulation mode particle concentrations were calculated in the CVS by a least square fit of the EEPS_6_CVS accumulation mode particle size distributions to a lognormal unimodal distribution, using only channels above 50 nm. EEPS nucleation mode particles were excluded from the fitting process since some of these channels were saturated and did not represent real values. In the fitting process, the lower and upper constraints of the geometric mean diameter were set as 30 nm and 200 nm, respectively. The broadness of the distribution is defined by the geometric standard deviation, which is the ratio of the diameter below which 84.1% of the particles are found to the geometric mean diameter (Seinfeld and Pandis 2006). The geometric standard deviations from the fitting process ranged from 1.4 to 1.9. The geometric mean diameters of the accumulation mode particles from the fitting process ranged from ∼50 nm to 127 nm. The three CPCs below the PMP tracked well with the accumulation mode concentrations of the EEPS_6_CVS until t = 320 s, indicating both the PMP systems remove semivolatile nucleation mode particles larger than 11 nm effectively.

The CPCs and the EEPS_6_CVS accumulation mode particle concentrations started to show discrepancies past the 320-s spike. While accumulation mode particle concentrations mea-

sured by the EEPS_6_CVS showed a minor increase from t = 325 s to t = 460 s, the CPC concentrations increased more than 10 times. These discrepancies will be discussed further in the Discussion section.

3.3. Particle Size Distributions Upstream and Downstream of the PMP Systems

It would also be very informative if particle size distributions could be measured downstream of the PMP. However, such measurements are extremely difficult to make due to the low particle concentrations under most conditions and the transient nature of the size distributions. Fortunately, particle size distributions upstream and downstream of the PMP system were measured simultaneously using two fast-response sizing instruments during the route 2 flow-of-traffic test in this study. The EEPS_6_CVS and f-SMPS_8 took samples at the CVS and downstream of the PMP system-A, respectively. Although the particle counts are at low levels, Figure 6 shows that the measurements were well above the lower limits of detection for the instruments. Particle size distributions measured at the CVS showed a bimodal distribution due to the presence of a nucleation mode, as shown in Figure 6a. It should be noted that the EEPS size channels from
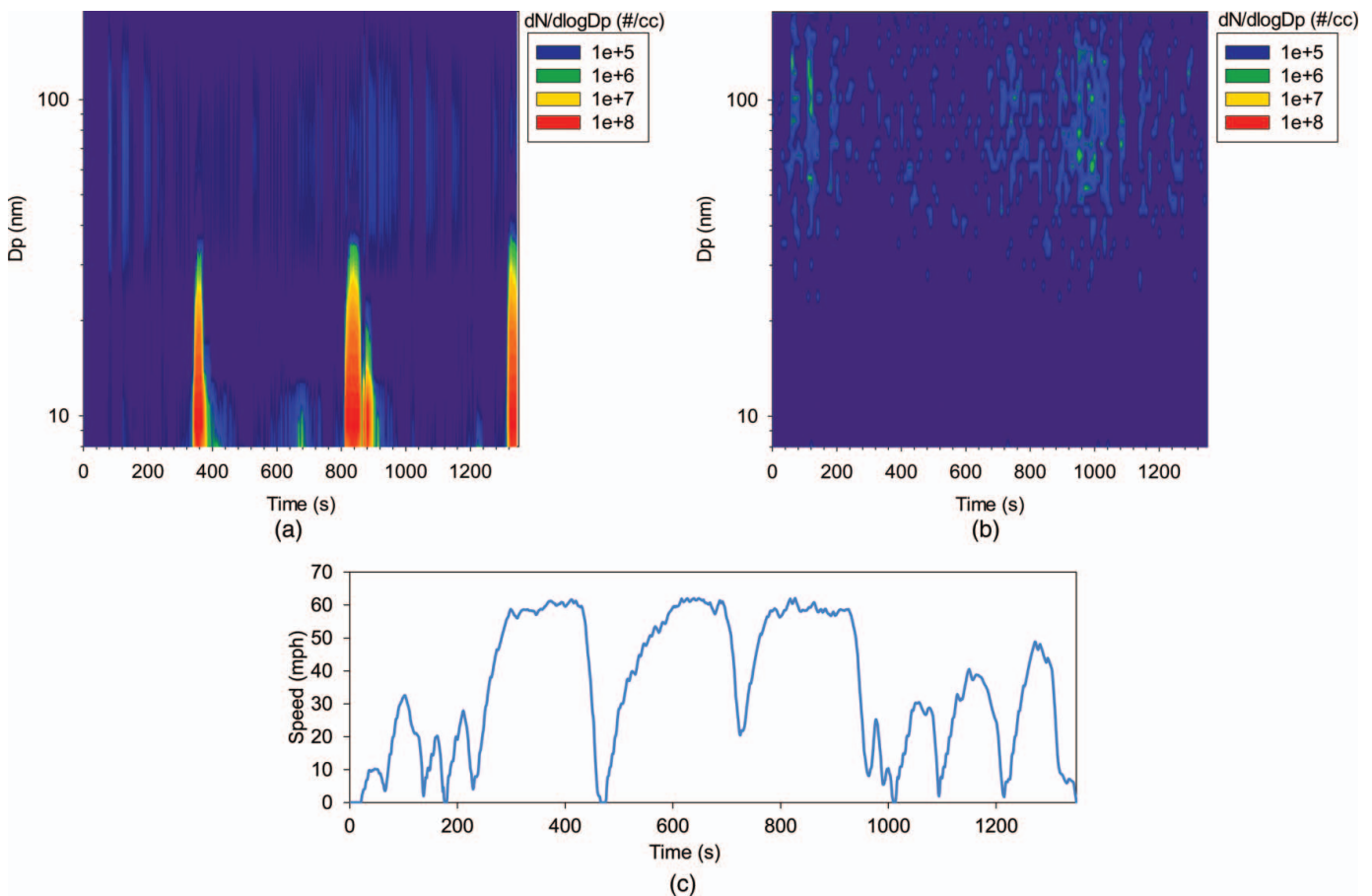

FIG. 6.   Comparison of particle size spectra from the CVS and PMP system during flow-of-traffic test (route 2): (a) particle size spectrum from the CVS using EEPS_6_CVS; (b) particle size spectrum from PMP system using fSMPS; (c) real-time vehicle speed. (Color figure available online.)

9 nm to 20 nm were saturated during the three nucleation mode particle formation events (i.e., t = 360, 840, and 1320 s). Particle size distributions downstream of the PMP system-A showed that accumulation mode particles passed through the PMP system, while semivolatile nucleation mode particles larger than 8 nm were effectively removed, as shown in Figure 6b. The vehicle speed is also plotted in Figure 6c. For the route 2 flow-of-traffic test, the fSMPS_8 data did not show a significant concentration of sub-11-nm particles downstream of the PMP, which is due to its relatively large cutoff diameter, 8 nm. The CPC_3_PMPA data, which are not presented here, but are reported in Johnson et al. (2009), did show the presence of sub-11-nm particles downstream of the PMP system. There was a slight difference in the geometric mean diameter of the accumulation mode measured by the two instruments. This is due to differences in the inversion algorithm between two instruments, multiple charge effects for a fractal-like aggregate (Bergmann et al. 2007), and the saturation of the EEPS channels in the nucleation mode size range.

4. DISCUSSION

4.1. Nature of Sub-23-nm Particles Downstream of the PMP Systems

The fact that there are a substantial number of sub-11-nm particles downstream of the PMP systems is consistent with the findings of Herner et al. (2007). They found 25–75% of the operationally defined solid particles under the PMP, measured by the EEPS, to be below 20 nm. Giechaskiel et al. (2009) also reported that the concentration of nonvolatile particles below 23 nm was 15–45% higher than the nonvolatile particles greater than 23 nm. These sub-23-nm particles found downstream of the PMP system are defined operationally as solid by the VPR's ability to remove semivolatile particles. However, the actual physical state of these operationally defined solid particles is unknown. It is important to understand the nature of these sub-23-nm particles to make sure that the PMP methodology counts majority of solid particles. There are several possible explanations for our observation of operationally defined solid particles. Three such hypotheses are discussed below.

The first hypothesis is solid particle penetration. Hu et al. (2009) reported that DPFs reduced emissions of total trace elements by 85% and 95% for cruise and UDDS cycles, respectively. The highest total metal emission rate was 0.06 mg/km in Hu et al.'s (2009) study, which was from the Veh1-DPF1 configuration (i.e., a class 8 tractor with a 1998 Cummins M11 diesel engine [11 L] with a CRT^{TM}) and the UDDS cycle. In this case, the metal emissions were dominated by calcium (Ca) and zinc (Zn) based on their high-resolution inductively coupled plasma mass spectrometer analysis. Ash particle number emissions from the engine used in this study were estimated using the total metal emission rate from Hu et al.'s (2009) study. Assuming the worst-case scenario, the ash particle number emission rate was calculated to be only 5.5×10^{10} par-

ticles/km, if all particles were spherical with a diameter of 3 nm and were composed of only $CaSO_4$ (which has a lower density than $ZnSO_4$). In this scenario, the ash particle number concentration is the highest. The calculated ash particle emission rate for this scenario was two orders of magnitude less than the total particle number emission rate downstream of the PMP system-A, 4.6×10^{12} particles/km, as measured by the CPC_3_PMPA. Since the number of particles that could be solid ash particles is relatively small, this hypothesis does not seem plausible.

The second hypothesis is re-nucleation of semivolatile particles downstream of the PMP systems, most likely made of sulfur compounds. This hypothesis suggests these semivolatiles evaporate at the VPR and re-nucleate downstream of the PMP system. Biswas et al. (2009) and Grose et al. (2006) reported significant changes in particle composition due to DPFs. Sulfate compounds and hydrocarbons dominated the particle mass for a catalyzed DPF-equipped engine in their studies, while elemental carbon or soot was found at much lower levels. Zheng et al. (2011) calculated the sulfuric acid vapor concentration in the CVS needed to form 10^5 particles/cm^3 (10-nm particles) downstream of the PMP system for the same vehicle and aftertreatment systems as used in the present study. They showed that only a 0.02% conversion of the fuel sulfur would provide high enough sulfuric acid vapor concentrations.

The primary dilution ratio of the PMP system-A was varied to examine the hypothesis of re-nucleation of semivolatile particles over different UDDS cycles, since nucleation by sulfur compounds is a steep nonlinear function of dilution ratio. Prior studies (Abdul-Khalek et al. 1999, 2000; Shi and Harrison 1999; Wei et al. 2001) have shown that a small change in dilution ratio can have a significant change in nucleated particle size distributions.

The overall dilution ratio of the PMP system-A ranged from 300 to 1500, over the test sequence. A corresponding increase in the dilution ratio for the PMP system-B could not be achieved due to its inherent design, so the PMP system-B was used with its standard operating conditions. It was expected that some change in re-nucleation could occur over this dilution ratio range. The results for the high dilution test are provided in Figure 7a. Note the higher cutpoint CPCs, the CPC_11_PMPA, the CPC_23_PMPA, and the CPC_11_PMPB, tracked well, which was expected. The CPC_3_PMPA showed a much smoother response than the three high cutoff diameter CPCs (i.e., the CPC_11_PMPA, the CPC_23_PMPA, and the CPC_11_PMPB). This is due to the fact that the CPC_3_PMPA performs auto-running averaging depending on the concentration. The lower the concentration (due to higher dilution ratio), the longer the running average time, and correspondingly, the slower the instrument response (TSI 2002). In this particular test, a 200-s running average was performed by the CPC_3_PMPA built-in software. The CPC_3_PMPB did not fall into the auto-running average concentration range, and tracked the vehicle load change well (not shown in the figure for the sake of readability).
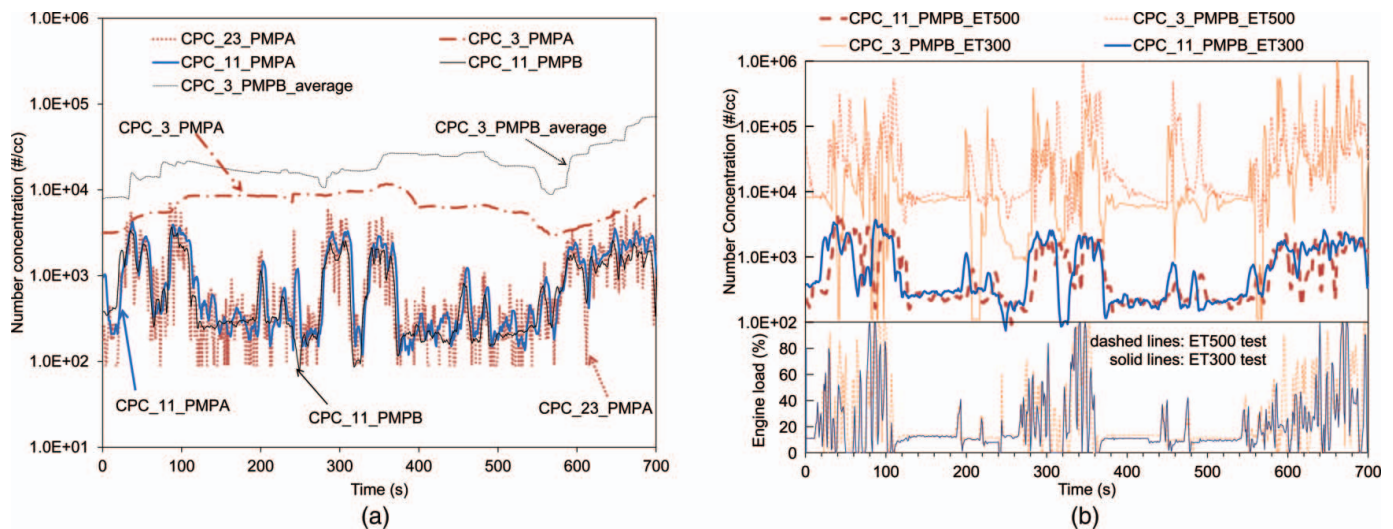
FIG. 7.   Particle concentrations under high-dilution and high-temperature conditions for the UDDS cycle: (a) PMP system-A at 1500 DR, PMP system B at 110 DR, a manual 200-s running average was performed for the CPC_3_PMPB to facilitate comparisons with the CPC_3_PMPA; (b) PMP system-B at VPR = 500°C and VPR = 300°C. (Color figure available online.)

To facilitate the comparison between the CPC_3_PMPA and the CPC_3_PMPB, a manual 200-s running average was performed for the CPC_3_PMPB, labeled as CPC_3_PMPB_average in Figure 7a. In contrast to the three high cutoff diameter CPCs, which agreed well for PMP system-A and -B, the concentrations of the CPC_3_PMPB_average were 20–90% higher than those of the CPC_3_PMPA, suggesting the re-nucleation of semivolatiles downstream PMP system-A was suppressed by the elevated dilution ratio. This high dilution test indicated that part, if not all, of the sub-23-nm particles downstream of the PMP systems were re-nucleated semivolatiles. It should be noted that vapors of semivolatiles would also condense onto the surfaces of accumulation particles downstream of the PMP systems, but condensation on existing particles does not change the particle number concentration. Thus, this second hypothesis appears to be a plausible explanation.

The third hypothesis is partial evaporation of large, less volatile particles. In another experiment, the ET temperature of the PMP system-B was increased to 500°C to examine this hypothesis (Figure 7b). The CPC_3_PMPB and CPC_11_PMPB concentrations of the high ET temperature test are labeled as CPC_3_PMPB_ET500 and CPC_11_PMPB_ET500 (dashed lines), respectively, in Figure 7b. The CPC_3_PMPB and CPC_11_PMPB concentrations from a similar test done at ET temperature of 300°C are also included in Figure 7b for better comparisons, labeled as CPC_3_PMPB_ET300 and CPC_11_PMPB_ET300 (solid lines), respectively. Engine loads of the two tests are plotted in Figure 7b as well. The CPC_11_PMPB_ET500 agreed well with the CPC_11_PMPB_ET300, indicating that the accumulation mode particles are not affected by the ET temperature variation. General agreement was seen between the CPC_3_PMPB_ET500 and

the CPC_3_PMPB_ET300 most of the time, except for a few occasions when the CPC_3_PMPB_ET300 concentrations fell to very low levels. It was noted that the CPC_3_PMPB_ET300 concentrations even fell below those of the CPC_11_PMPB_ET300 during these occasions, which is theoretically impossible. This was most likely due to an occasional clog of the aerosol capillary tube of the CPC_3_PMPB_ET300 (TSI, personal communication, 2012). If the operationally defined solid particles are due to incomplete evaporation of semivolatile particles, then one would expect a decrease in sub-11-nm particle concentrations when the PMP ET is operated at elevated temperatures. Such a response was not observed in this test, as discussed earlier. Thus, the partial evaporation hypothesis does not seem possible.

4.2.   Implications to On-Road Flow-of-Traffic Driving

Several other measurements and observations that were made during the test, but not presented here, are worth mentioning to fully understand the discrepancy between the EEPS_6_CVS accumulation mode particle concentration and the much higher CPC concentrations from t = 325 s to t = 460 s. These measurements and observations during this time period are: (a) the EEPS_6_CVS total particle concentrations were flat; (b) nine EEPS_6_CVS channels, from 9.3 nm to 29.4 nm, were saturated; (c) both the TSI Dustrak and Dekati mass monitor (DMM) measuring in the CVS showed about a 50% increase in particle mass concentrations; and (d) total hydrocarbon (THC) mass concentrations increased more than one order of magnitude based on the THC measurement. These observations, along with only a slight increase in the EEPS_6_CVS accumulation mode particle concentrations, suggest a large increase in nucleation mode particles that was not captured by the EEPS_6_CVS because some of the nucleation mode size channels were saturated.

Given these observations, the differences between the EEPS_6_CVS accumulation mode particle concentration and the much higher CPC concentrations can be attributed to the growth of re-nucleated semivolatile particles downstream of the PMP systems. After formation by nucleation, some of the particles grew larger than 11 nm and others even grew larger than 23 nm, causing the difference between the three high cutoff diameter CPCs and the EEPS_6_CVS accumulation mode particle concentrations. The differences would have been even greater, but the concentrations of these re-nucleated semivolatile particles were so high that all the three CPCs were saturated during this period of time. It is acknowledged that dilution ratios should have been adjusted to avoid instrument saturation. Resources were not available to repeat the test with higher dilution ratios, however. Dwyer et al. (2010) also observed a sharp increase in PMP operationally defined solid particles during a DPF regeneration event for a light-duty diesel vehicle and proposed that the incomplete removal of semivolatile particles by the PMP could contribute to the sharp increase in apparently solid particles. However, as indicated by the current study, and given the existence of high concentrations of volatile or semivolatile nucleation mode particles during DPF regeneration (Mamakos and Martini 2011), the sharp increase in the operationally defined solid particles in Dwyer et al.'s (2010) study was probably due to re-nucleated particles that grew larger than the 23-nm size cut.

5. CONCLUSIONS

The objective of this study was to evaluate the performance of the European PMP methodology for the measurement of solid particle number emissions under different driving conditions. The testing was conducted using a heavy-duty vehicle equipped with a passive DPF and CE-CERT's MEL. Emissions measurements were conducted over a series of standard driving cycles, including the UDDS and the motorway segment of the European ETC cycle, as well as under two on-road, flow-of-traffic conditions.

For the ETC motorway cycle, a nucleation event was observed in the CVS near the beginning of the cycle, which was attributed to the acceleration prior to starting the test cycle. These nucleation mode particles rapidly decreased as the cycle continued but decreased in size to smaller than 6 nm. Nucleation mode particles smaller than 6 nm were also observed in the CVS during the more transient UDDS cycle. During the route 1 flow-of-traffic test, where the average engine load was higher than that during the standard testing cycle, total particle number concentrations in the CVS were dominated by the nucleation mode particles. For the same flow-of-traffic test, accumulation mode particle concentrations were orders of magnitude higher than those of the standard testing cycles.

Overall, particle concentrations measured by the PMP-compliant CPC (model 3790 with a cutoff diameter of 23 nm) corresponded well with different engine loads and accumulation mode particle concentrations for all the testing cycles conducted. The CPCs with cutoff diameters of 11 nm tracked well with the CPC with the cutoff diameter of 23 nm downstream of the PMP systems, indicating limited numbers of particles between 11 and 23 nm. However, CPCs with the smallest cutoff diameter of 3 nm always measured higher concentrations than other CPCs, showing the presence of a significant number of sub-11-nm particles downstream of the PMP systems. Two different PMP systems used in this study showed no distinguishable difference in terms of CPC responses.

We hypothesize that the majority of the particles in the sub-11-nm size range were formed from re-nucleation of vaporized semivolatile particles in the ET and were not truly solid, as indicated by the reduced number concentration of sub-11-nm particles downstream of the PMP system at an elevated PMP dilution ratio. It is worth mentioning that a follow-up study by Zheng et al. (2011), which includes more fundamental experiments, did show that some truly solid particles can be formed in the ET from mixtures of semivolatile hydrocarbon and sulfuric acid particles. During a UDDS cycle, when the ET temperature was increased from 300°C to 500°C, no difference in particle number concentrations was observed, suggesting that incomplete evaporation of semivolatile particles did not contribute to those sub-11-nm particles. It was shown by a calculation based on metal particle emission factors from Hu et al. (2009) that worst-case metal ash particle concentrations would be approximately two orders of magnitude less than the total particle number concentrations downstream of the PMP system, suggesting that these particles were not solid particles with ash origin.

During the route 1 flow-of-traffic test, a sudden jump of about two orders of magnitude in particle number concentrations measured by the PMP-compliant CPC was observed. This was attributed to the extensive growth of the re-nucleated artifact particles downstream of the PMP systems, which in turn was associated with a very high concentration of hydrocarbons in the exhaust. Although there concentrations are well above typical operating conditions for the PMP, this also suggests that quantifying solid particle concentrations in situations where very high semivolatile particle concentrations might be found, such as regeneration, could be challenging.

REFERENCES

Abdul-Khalek, I., Kittelson, D. B., and Brear, F. (1999). The Influence of Dilution Conditions on Diesel Exhaust Particle Size Distribution Measurements. *SAE Trans.*, 108:563–571.

Abdul-Khalek, I., Kittelson, D. B., and Brear, F. (2000). Nanoparticle Growth During Dilution and Cooling of Diesel Exhaust: Experimental Investigation and Theoretical Assessment. *SAE Technical Papers Series 2000-01-0515.* SAE International, Warrendale, PA.

Andersson, J., Giechaskiel, B., Muñoz-Bueno, R., Sandbach, E., and Dilara, P. (2007). Particle Measurement Programme (PMP) Light-Duty Inter-Laboratory Correlation Exercise (ILCE_LD) Final Report from European Commission Joint Research Center.

Andersson, J., Mamakos, A., Giechaskiel, B., Carriero, M., and Martini, G. (2010). Particle Measurement Programme (PMP) Heavy-Duty Inter-Laboratory Correlation Exercise (ILCE_HD) Final Report from European Commission Joint Research Center.

Bergmann, M., Scheer, V., Vogt, R., and Benter, T. (2007). Comparison of the Performance of Real-Time PM Mass and Number Instrumentation for Vehicle Exhaust Measurements. *SAE Technical Paper Series 2007-24-0116*. SAE International, Warrendale, PA.

Biswas, S., Verma, V., Schauer, J. J., and Sioutas, C. (2009). Chemical Speciation of PM Emissions from Heavy-Duty Diesel Vehicles Equipped with Diesel Particulate Filter (DPF) and Selective Catalytic Reduction (SCR) Retrofits. *Atmos. Environ.*, 43:1917–1925.

Burtscher, H. (2005). Physical Characterization of Particulate Emissions from Diesel Engines: A Review. *J. Aerosol. Sci.*, 36:896–932.

Chase, R. E., Duszkiewicz, G. J., Richert, J. F. O., Lewis, D., Maricq, M. M., and Xu, N. (2004). PM Measurement Artifact: Organic Vapor Deposition on Different Filter Media. *SAE Technical Paper Series 2004-01-0967*. SAE International, Warrendale, PA.

Durbin, T. D., Jung, H., Cocker, D. R., Johnson, K., and Chaudhary, A. (2008). *Evaluation of the Proposed New European Methodology for Determination of Particle Number Emissions and Its Potential in California for In-Use Screening*, California Air Resources Board, Sacramento, CA.

Dwyer, H., Ayala, A., Zhang, S., Collins, J., Huai, T., Herner, J., et al. (2010). Emissions from a Diesel Car During Regeneration of an Active Diesel Particulate Filter. *J. Aerosol. Sci.*, 41:541–552.

EPA (2002). Health Assessment Document For Diesel Engine Exhaust. Report from US Environmental Protection Agency.

Filippo, A. D., and Maricq, M. M. (2008). Diesel Nucleation Mode Particles: Semivolatile or Solid? *Environ. Sci. Technol.*, 42:7957–7962.

Giechaskiel, B., Dilara, P., and Andersson, J. (2008). Particle Measurement Programme (PMP) Light-Duty Inter-Laboratory Exercise: Repeatability and Reproducibility of the Particle Number Method. *Environ. Sci. Technol.*, 42:528–543.

Giechaskiel, B., Carriero, M., Martini, G., and Andersson, J. (2009). Heavy Duty Particle Measurement Programme (PMP): Exploratory Work for the Definition of the Test Protocol. *SAE Technical Paper Series 2009-01-1767*. SAE International, Warrendale, PA

Grose, M., Sakurai, H., Savstrom, J., Stolzenburg, M. R., Watts Jr, W. F., Morgan, C. G., et al. (2006). Chemical and Physical Properties of Ultrafine Diesel Exhaust Particles Sampled Downstream of a Catalytic Trap. *Environ. Sci. Technol.*, 40:5502–5507.

Herner, J. D., Hu, S., Robertson, W. H., Huai, T., Chang, M. C. O., Rieger, P., et al. (2011). Effect of Advanced Aftertreatment for PM and NO$_x$ Reduction on Heavy-Duty Diesel Engine Ultrafine Particle Emissions. *Environ. Sci. Technol.*, 45:2413–2419.

Herner, J. D., Robertson, W. H., and Ayala, A. (2007). Investigation of Ultrafine Particle Number Measurements from a Clean Diesel Truck Using the European PMP Protocol. *SAE Technical Paper Series 2007-01-1114*. SAE International, Warrendale, PA.

Hu, S., Herner, J. D., Shafer, M., Robertson, W., Schauer, J. J., Dwyer, H., et al (2009). Metals Emitted from Heavy-Duty Diesel Vehicles Equipped with Advanced PM and NO$_X$ Emission Controls. *Atmos. Environ.*, 43: 2950–2959.

Johnson, K. C., Durbin, T. D., Jung, H., Chaudhary, A., Cocker, D. R., Herner, J. D., et al. (2009). Evaluation of the European PMP Methodologies During On-Road and Chassis Dynamometer Testing for DPF Equipped Heavy-Duty Diesel Vehicles. *Environ. Sci. Technol.*, 43:962–969.

Kittelson, D. B., Watts, W. F., and Johnson, J. P. (2006). On-Road and Laboratory Evaluation of Combustion Aerosols–Part1: Summary of Diesel Engine Results. *J. Aerosol. Sci.*, 37:913–930.

Lähde, T., Rönkkö, T., Virtanen, A., Schuck, T. J., Pirjola, L., Hämeri, K., et al. (2009). Heavy Duty Diesel Engine Exhaust Aerosol Particle and Ion Measurements. *Environ. Sci. Technol.*, 43:163–168.

Lähde, T., Rönkkö, T., Virtanen, A., Solla, A., Kytö, M., Söderström, C., et al. (2010). Dependence between Nonvolatile Nucleation Mode Particle and Soot Number Concentrations in an EGR Equipped Heavy-Duty Diesel Engine Exhaust. *Environ. Sci. Technol.*, 44:3175–3180.

Li, R., Ning, Z., Cui, J., Khalsa, B., Ai, L., Takabe, W., et al. (2009). Ultrafine Particles from Diesel Engines Induce Vascular Oxidative Stress via JNK Activation. *Free Radical. Bio. Med.*, 46:775–782.

Mamakos, A., and Martini, G. (2011). *Particle Number Emissions During Regeneration of DPF-Equipped Light Duty Diesel Vehicles: A Literature Survey*, European Commission Joint Research Centre, Brussels.

Rönkkö, T., Virtanen, A., Kannosto, J., Keskinen, J., Lappi, M., and Pirjola, L. (2007). Nucleation Mode Particles with a Nonvolatile Core in the Exhaust of a Heavy Duty Diesel Vehicle. *Environ. Sci. Technol.*, 41:6384–6389.

Seinfeld, J. H., and Pandis, S. N. (2006). *Atmospheric Chemistry and Physics: From Air Pollution to Climate Change*. John Wiley & Sons, New York.

Shah, S., and Cocker, D. R. (2005). A Fast Scanning Mobility Particle Spectrometer for Monitoring Transient Particle Size Distributions. *Environ. Sci. Technol.*, 39:519–526.

Shi, J. P., and Harrison, R. M. (1999). Investigation of Ultrafine Particle Formation during Diesel Exhaust Dilution. *Environ. Sci. Technol.*, 33: 3730–3736.

Swanson, J., Kittelson, D., and Dikken, D. (2009). Uncertainties in Filter Mass Measurements Made to Determine Compliance with the 2007 Diesel PM Standard. *SAE Technical Paper Series 2009-01-1516*. SAE International, Warrendale, PA.

TSI. (2002). Model 3025A Ultrafine Condensation Particle Counter Instruction Manual.

Wei, Q., Kittelson, D. B., and Watts, W. F. (2001). Single-stage dilution tunnel performance. *SAE Technical Paper Series 2001-01-0201*. SAE International, Warrendale, PA

Zheng, Z., Johnson, K. C., Liu, Z., Durbin, T. D., Hu, S., Huai, T., et al. (2011). Investigation of Solid Particle Number Measurement: Existence and Nature of Sub-23 nm Particles under PMP Methodology. *J. Aerosol. Sci.*, 42:883–897.